

Improvement in Aluminum Complexes Bearing Schiff Base in Ring-Opening Polymerization of ϵ -Caprolactone: The Synergy of N,S-Schiff Base in a Five-Membered Ring Aluminum System

Ting-Wei Huang,^a Rou-Rong Su,^a Yi-Chen Lin,^a Hsin-Yu Lai,^a Chien-Yi Yang,^a Gopal Chandru Senadi,^b Yi-Chun Lai,^a Michael Y. Chiang,^{ac} Hsuan-Ying Chen^{*acd}

^a Department of Medicinal and Applied Chemistry, Kaohsiung Medical University, Kaohsiung, Taiwan, 80708, Republic of China

^b Department of Chemistry, SRM Research Institute, SRM University, Kattankulathur 603 203, Chennai, Tamilnadu, India

^c Department of Chemistry, National Sun Yat-Sen University, Kaohsiung, 80424, Republic of China

^d Department of Medical Research, Kaohsiung Medical University Hospital, Kaohsiung 80708, Republic of China

Electronic supplementary information available: Polymer characterization data, and details of the kinetic study.

Table of Contents

Table S1.	The kinetic study of polymerizations of ϵ -caprolactone using various Al complexes as catalysts.....	2
Table S2.	The kinetic study of polymerizations of ϵ -caprolactone using various concentration of $\text{L}^{\text{ClBr}}\text{AlMe}_2$ as a catalyst.....	3
Tables S3-S7	The X-ray crystallography data of $\text{L}^{\text{CH}}\text{AlMe}_2$ (4).....	16-22
Figure S1	First-order kinetic plots of CL polymerizations with various $[\text{L}^{\text{ClBr}}\text{-AlMe}_2 + 2 \text{BnOH}]$ plotted against time.....	4
Figure S2-S16.	^1H NMR and ^{13}C spectra of all Al complexes.....	5-12
Figure S17.	MALDI-TOF spectrum of PCL (matrix: DCTB; ionization salt: NaI; solvent: CH_2Cl_2 , entry 9, Table 3).....	12
Figure S18-S22.	^1H NMR and ^{13}C spectra of all crude ligands.....	13-15

Details of the Kinetic Study of ε -Caprolactone Polymerization

A typical kinetic study was conducted to establish the reaction order with respect to monomer and various Al complexes. For CL polymerization, ε -caprolactone (1.14g, 0.01 mol) was added to a solution of the mixture of Al complexes (0.1 mmol) and BnOH (0.02 mmol) in toluene (5 mL), respectively. The solution was then stirred at room temperature under nitrogen. At the indicated time intervals, 0.05 mL aliquots were removed, trapped with CDCl_3 (1mL), and analyzed by ^1H NMR. The ε -caprolactone concentration [CL] was determined by integrating the triplet methylene peak of CL at 4.20 ppm and the triplet methylene peak of polylactone at 4.00 ppm. As expected, plots of $\ln([CL]_0/[CL])$ vs. time for a wide range of Al complexes are linear, indicating the usual first order dependence on monomer concentration (Figures 4, Table S1). Thus, the rate expression can be written as $-d[CL]/dt = k_{\text{obs}}[CL]^1$, where $k_{\text{obs}} = k_{\text{app}}[\text{Al complex} + 2 \text{BnOH}]^x$. A plot of (k_{obs}) vs. [$\text{Al complex} + 2 \text{BnOH}$] (Figure S1, Table S2) is linear, indicating the order of [$\text{Al complex} + 2 \text{BnOH}$] ($x = 1$) and k_{app} which is $0.296 \text{ M}^{-1}\text{min}^{-1}$.

Table S1. The kinetic study of polymerizations of ε -caprolactone using various Al complexes as catalysts

Time/min	$\text{L}^{\text{Cibr}}\text{AlMe}_2$	$\text{L}^{\text{ClCl}}\text{AlMe}_2$	$\text{L}^{\text{CIH}}\text{AlMe}_2$	$\text{L}^{\text{HH}}\text{AlMe}_2$	$\text{L}^{\text{ClO}}\text{AlMe}_2$
Conversion of PCL					
2	0.34	0.10	0.10	0.09	
4	0.55	0.33	0.29	0.26	0.085
6	0.78	0.67	0.50	0.51	0.25
8	0.86	0.83	0.64	0.60	
10		0.89	0.73	0.67	0.54
12	0.96	0.92	0.78		0.67
20			0.92	0.80	0.86
25				0.95	0.90
30					0.94
k_{obs}	0.284 (12)	0.260 (17)	0.136 (4)	0.115 (8)	0.105 (4)
Induction period/min	0.83 (31)	1.79 (51)	0.94 (34)	0.78 (102)	2.60 (69)
R^2	0.997	0.992	0.997	0.986	0.996

Table S2. The kinetic study of polymerizations of ϵ -caprolactone using various concentrations of $\text{L}^{\text{ClBr}}\text{AlMe}_2$ as a catalyst and BnOH as an initiator

Time (min)	$[\text{L}^{\text{ClBr}}\text{AlMe}_2 + 2 \text{ BnOH}]$				
	5 mM	10 mM	20 mM	25 mM	30 mM
2			0.34	0.22	0.32
3		0.071			
4			0.55	0.52	0.69
6		0.13	0.78	0.76	0.87
8			0.86	0.87	0.95
10		0.23		0.94	
15		0.34	0.96		
20		0.47			
30	0.087	0.65			
60	0.16	0.93			
120	0.32				
150	0.42				
180	0.49				
210	0.56				
253	0.65				
373	0.82				
$k_{\text{obs}} \times 10^3$	4.76 (21)	36.54 (18)	284.14 (1221)	321.81(1346)	434.96(1344)
Induction period/min	28	2	1	1	1
R^2	0.994	0.995	0.997	0.997	0.999

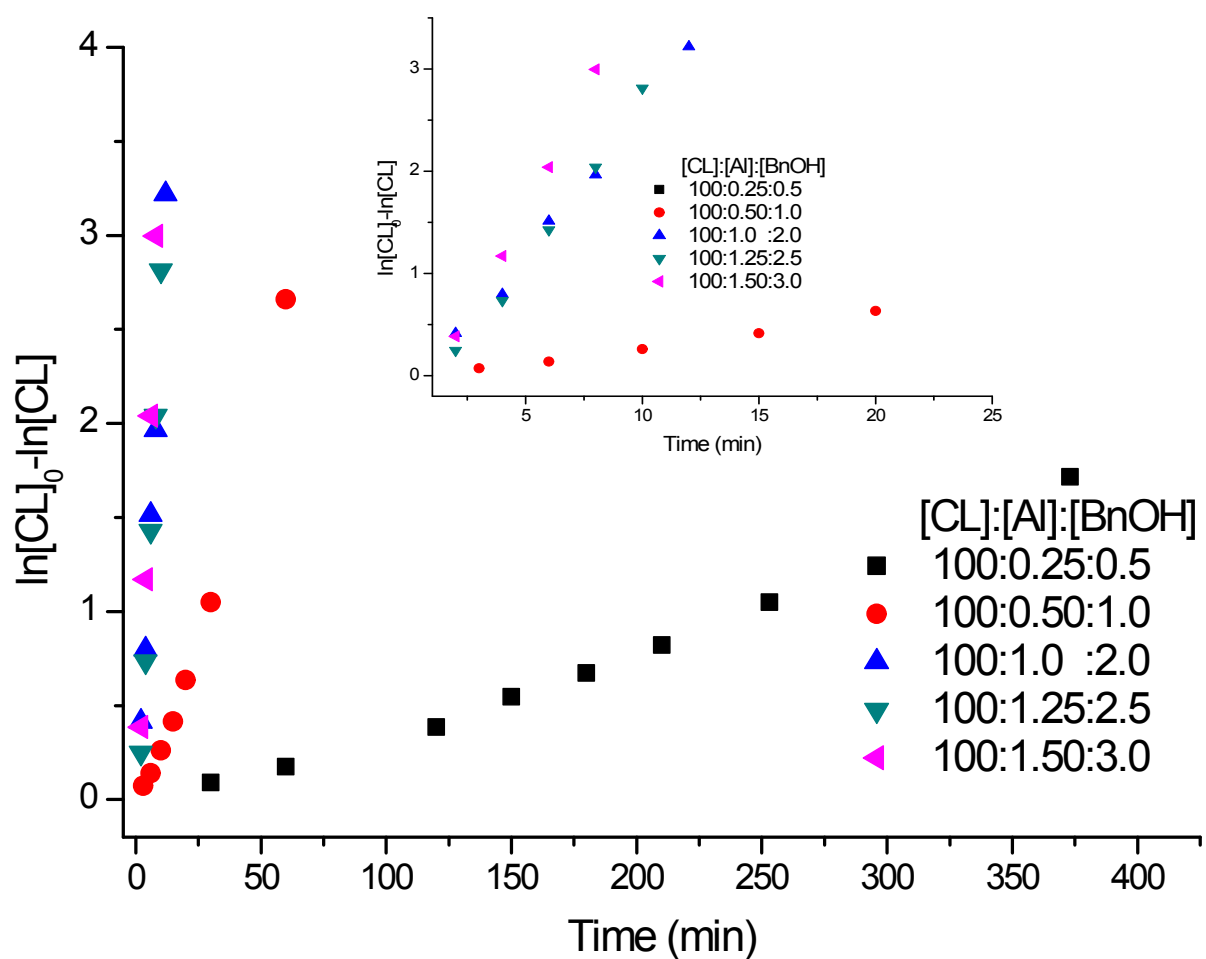


Figure S1. First-order kinetic plots of CL polymerization with various concentrations of $[\text{L}^{\text{ClBr}}\text{AlMe}_2 + 2 \text{BnOH}]$ plotted against time with $[\text{CL}] = 2.0 \text{ M}$ in toluene 5 mL

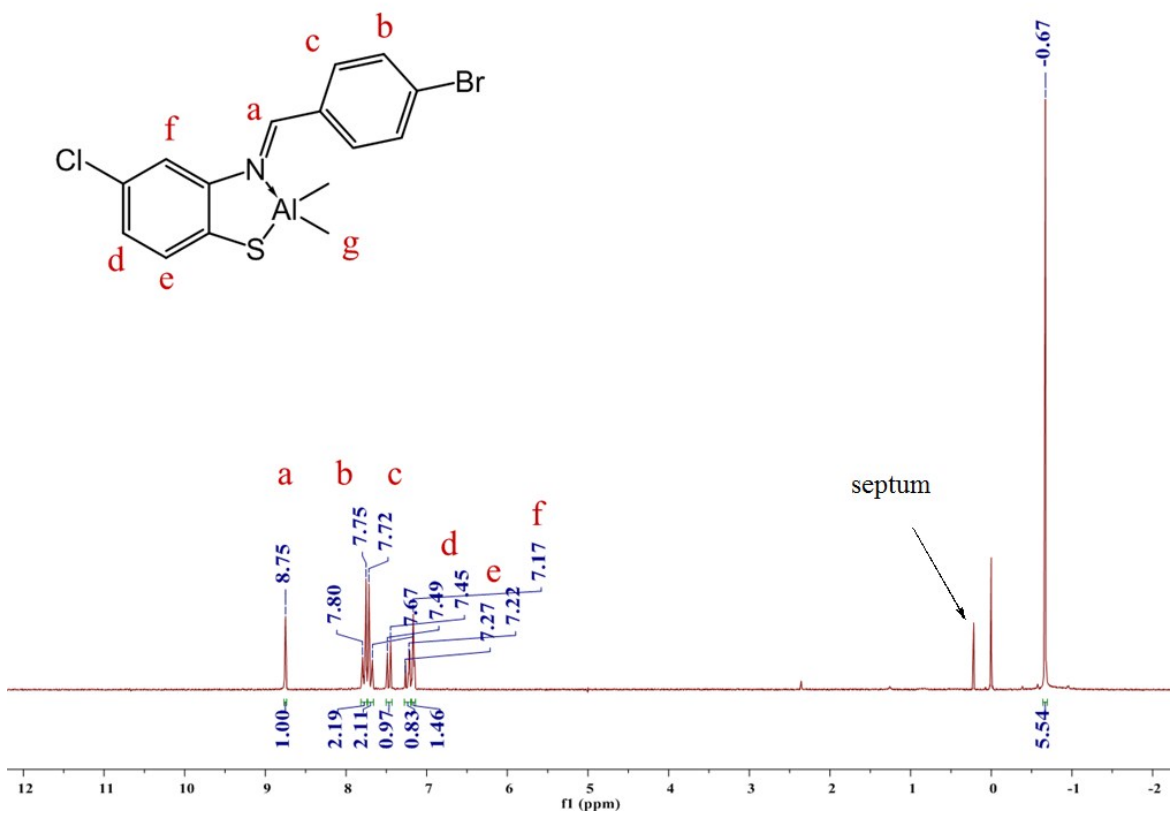


Figure S2. ^1H NMR spectrum of $\text{L}^{\text{ClBr}}\text{AlMe}_2$

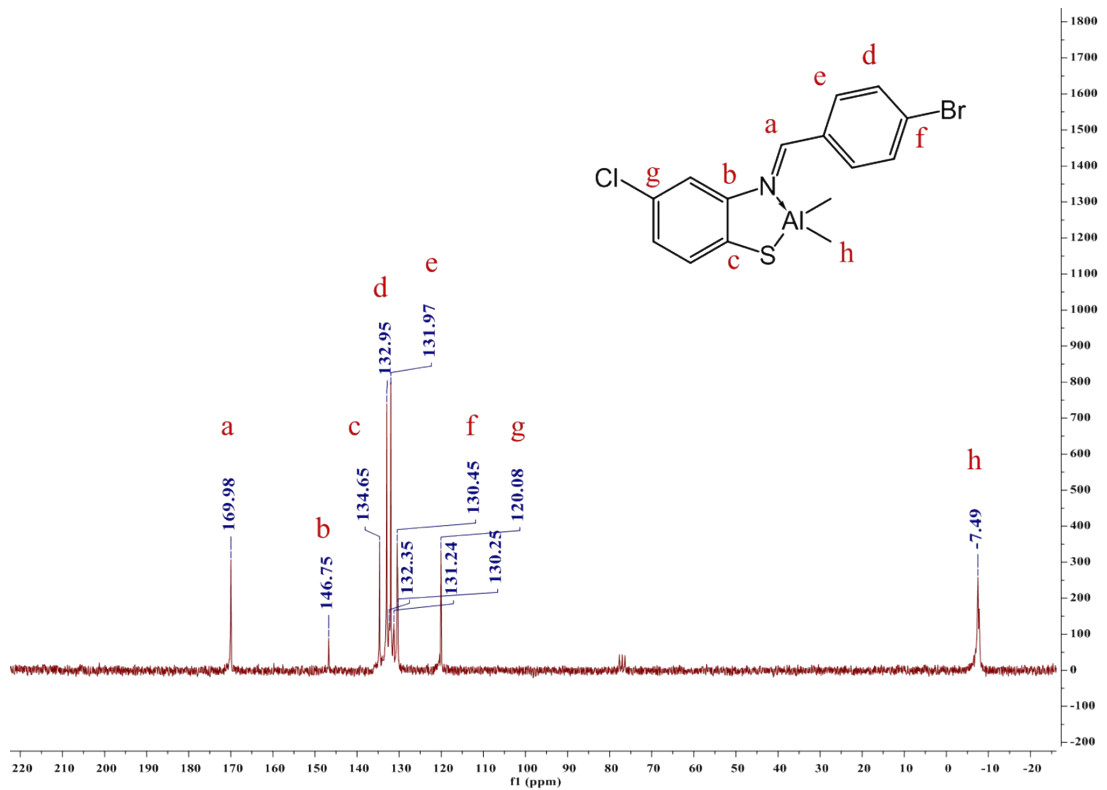


Figure S3. ^{13}C NMR spectrum of $\text{L}^{\text{ClBr}}\text{AlMe}_2$

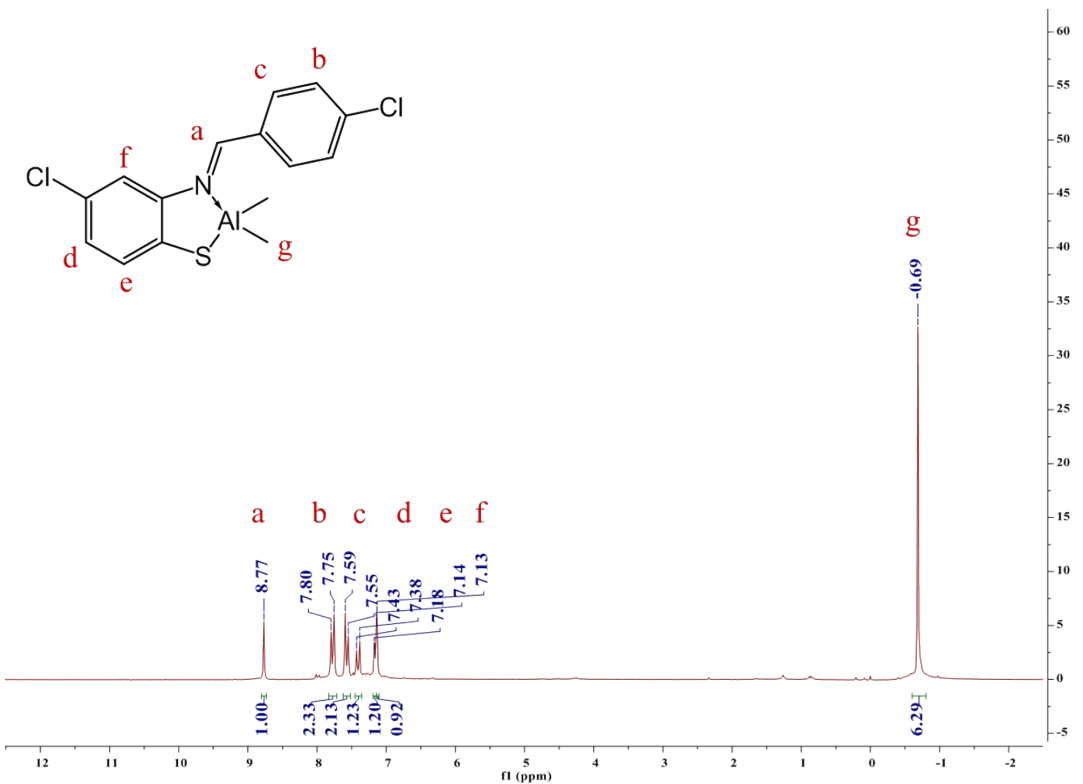


Figure S4. ^1H NMR spectrum of $\text{L}^{\text{Cl}}\text{AlMe}_2$

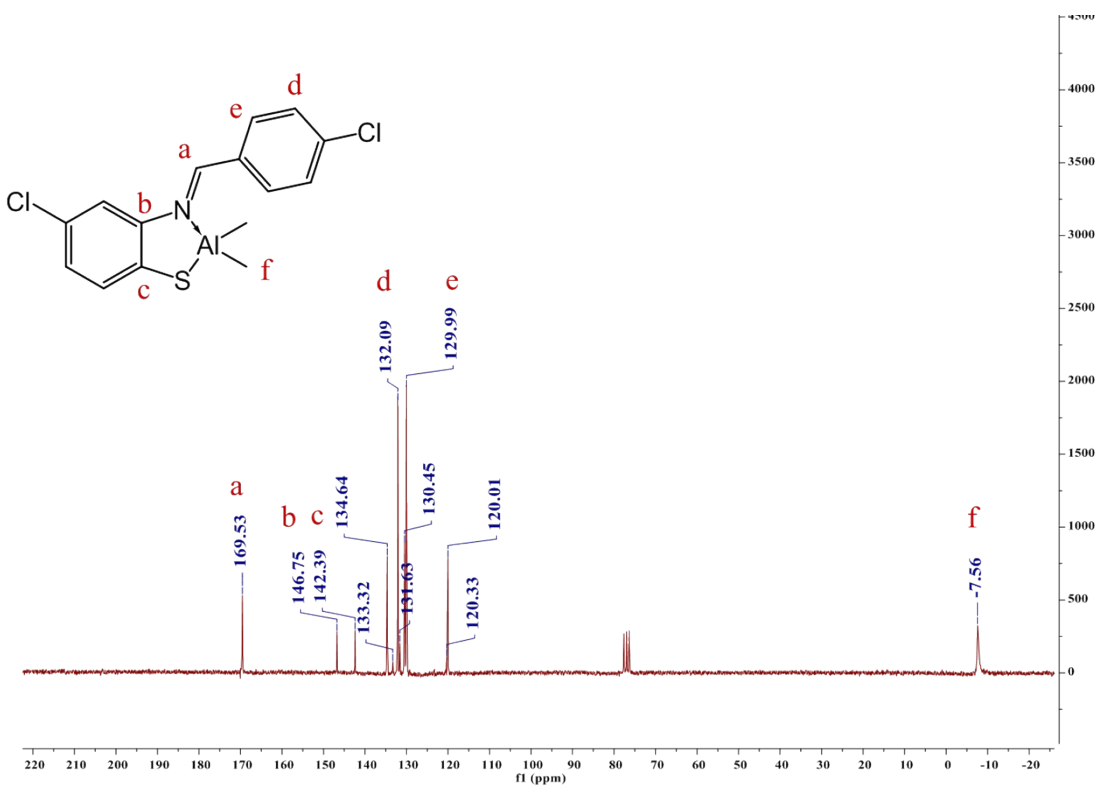


Figure S5. ^{13}C NMR spectrum of $\text{L}^{\text{Cl}}\text{AlMe}_2$

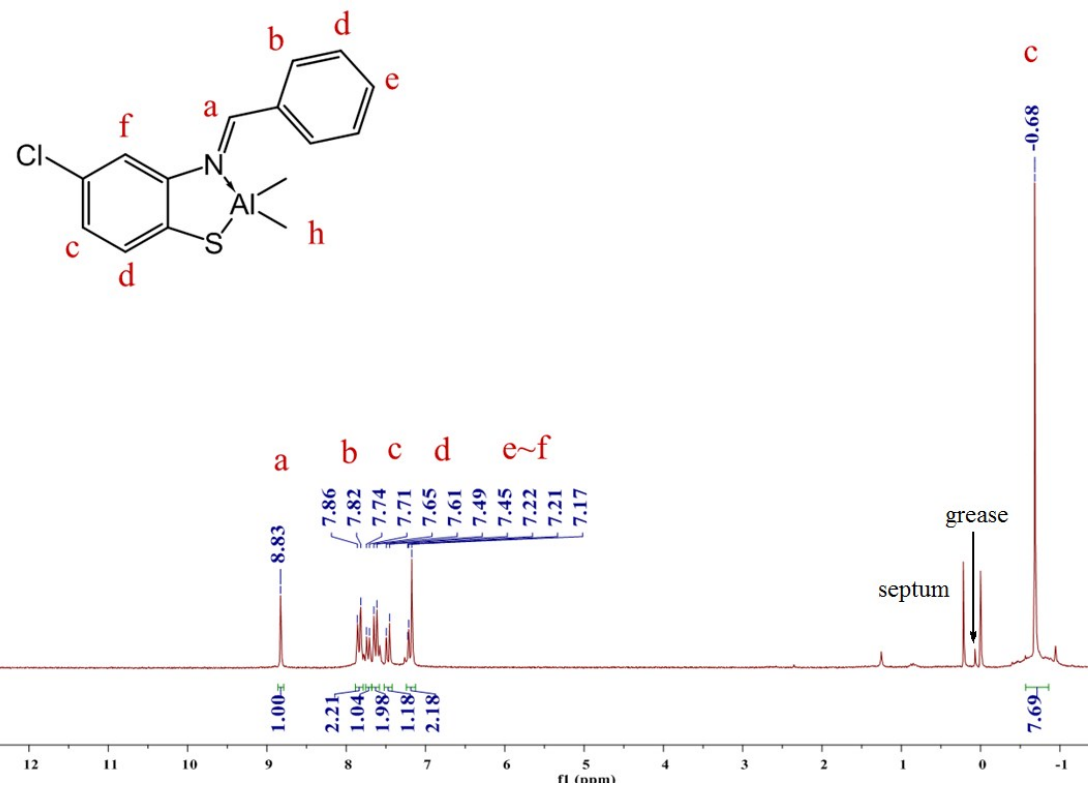


Figure S6. ¹H NMR spectrum of $\text{L}^{\text{ClH}}\text{AlMe}_2$

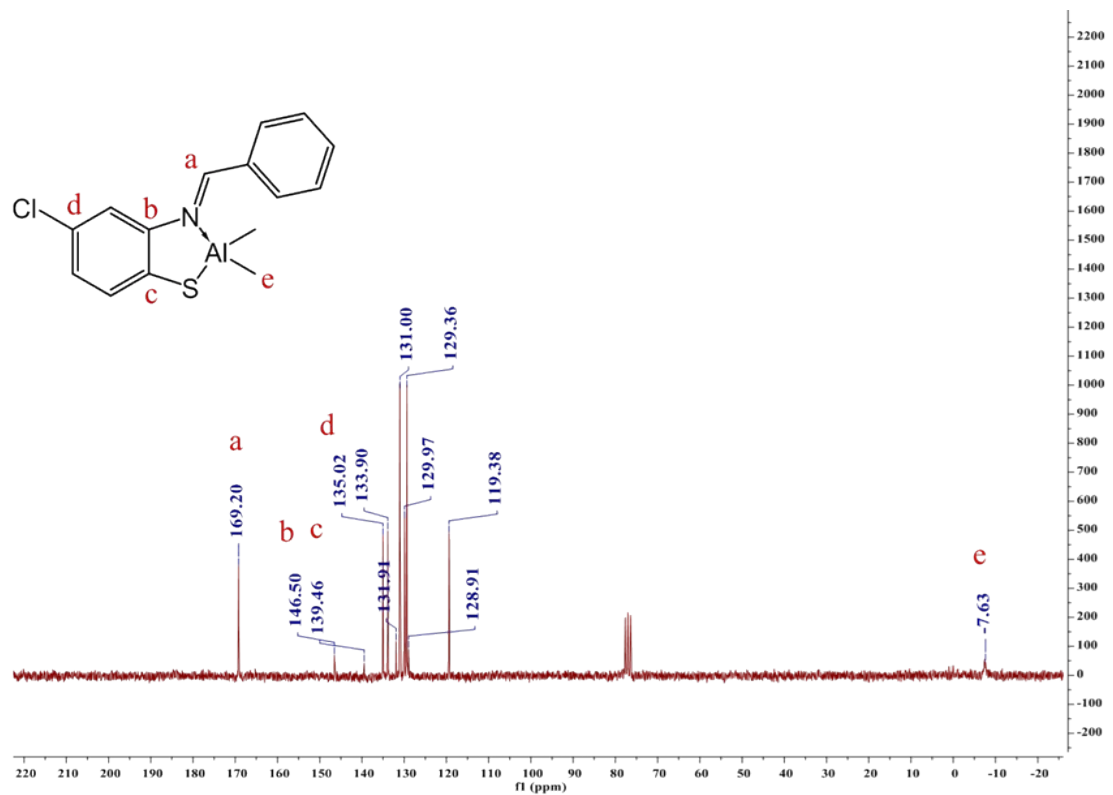


Figure S7. ¹³C NMR spectrum of $\text{L}^{\text{ClH}}\text{AlMe}_2$

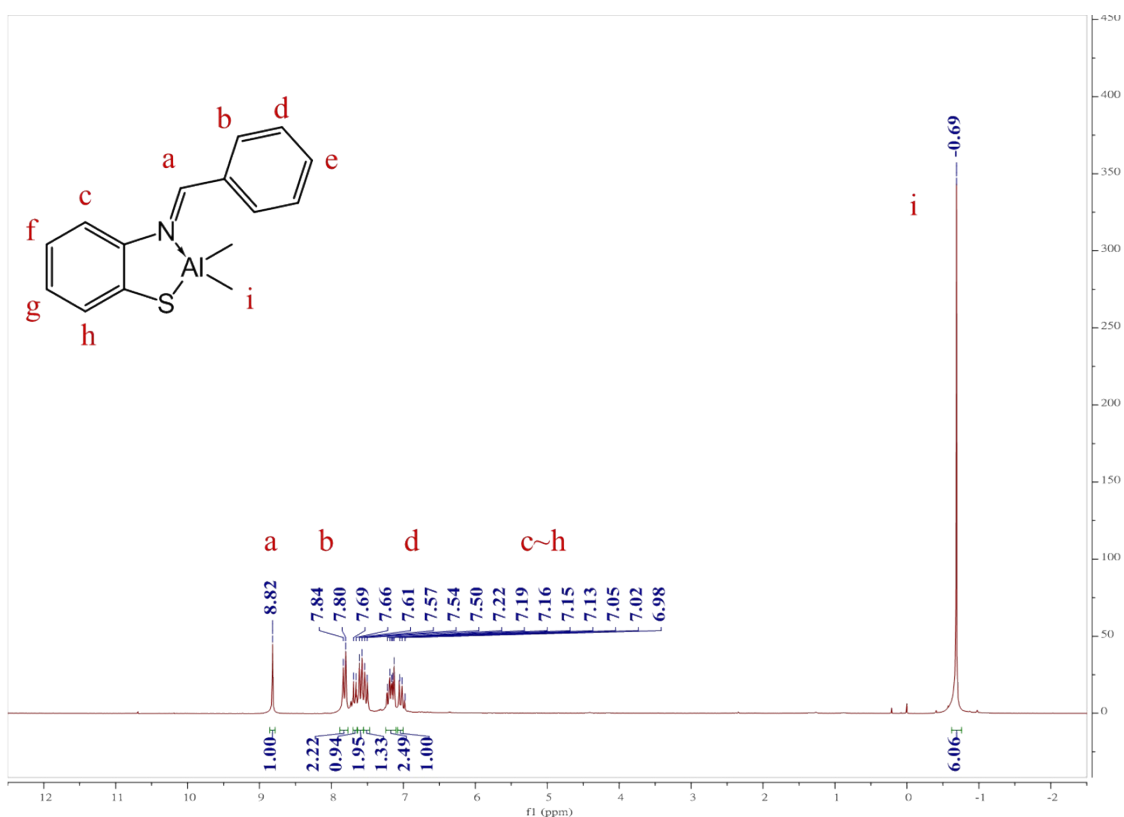


Figure S8. ¹H NMR spectrum of $\text{L}^{\text{HH}}\text{AlMe}_2$

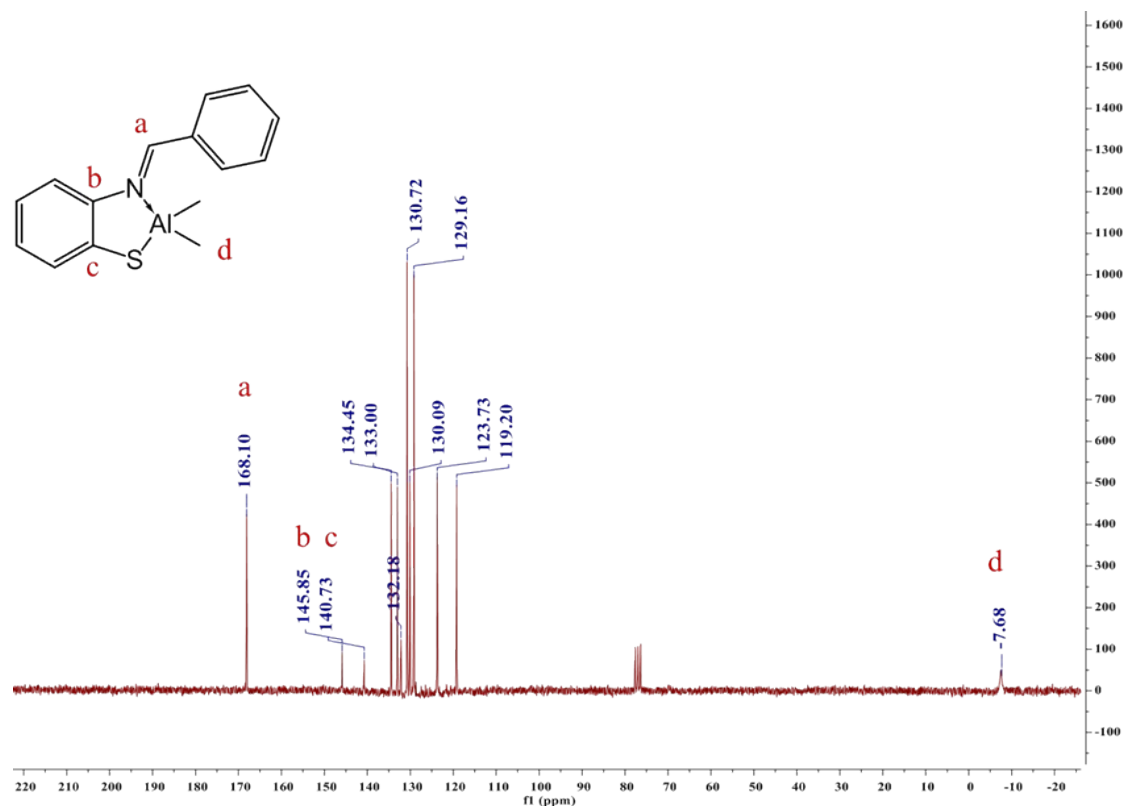


Figure S9. ¹³C NMR spectrum of $\text{L}^{\text{HH}}\text{AlMe}_2$

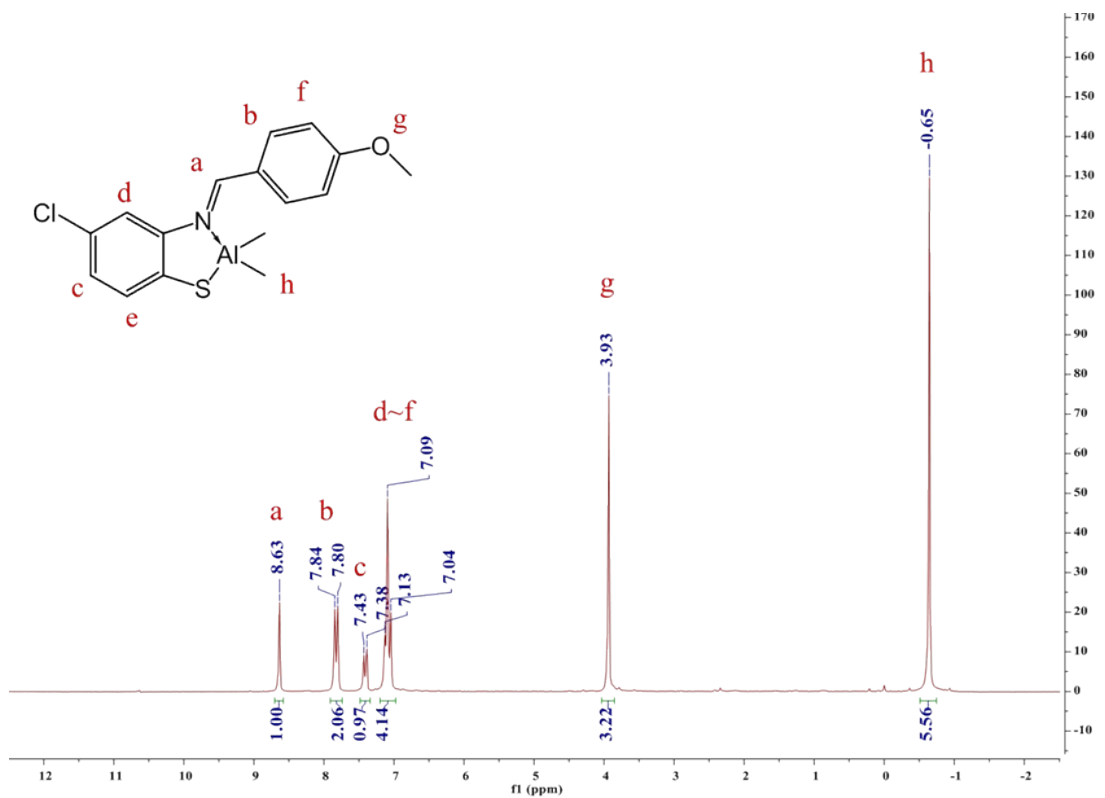


Figure S10. ${}^1\text{H}$ NMR spectrum of $\text{L}^{\text{ClO}}\text{AlMe}_2$

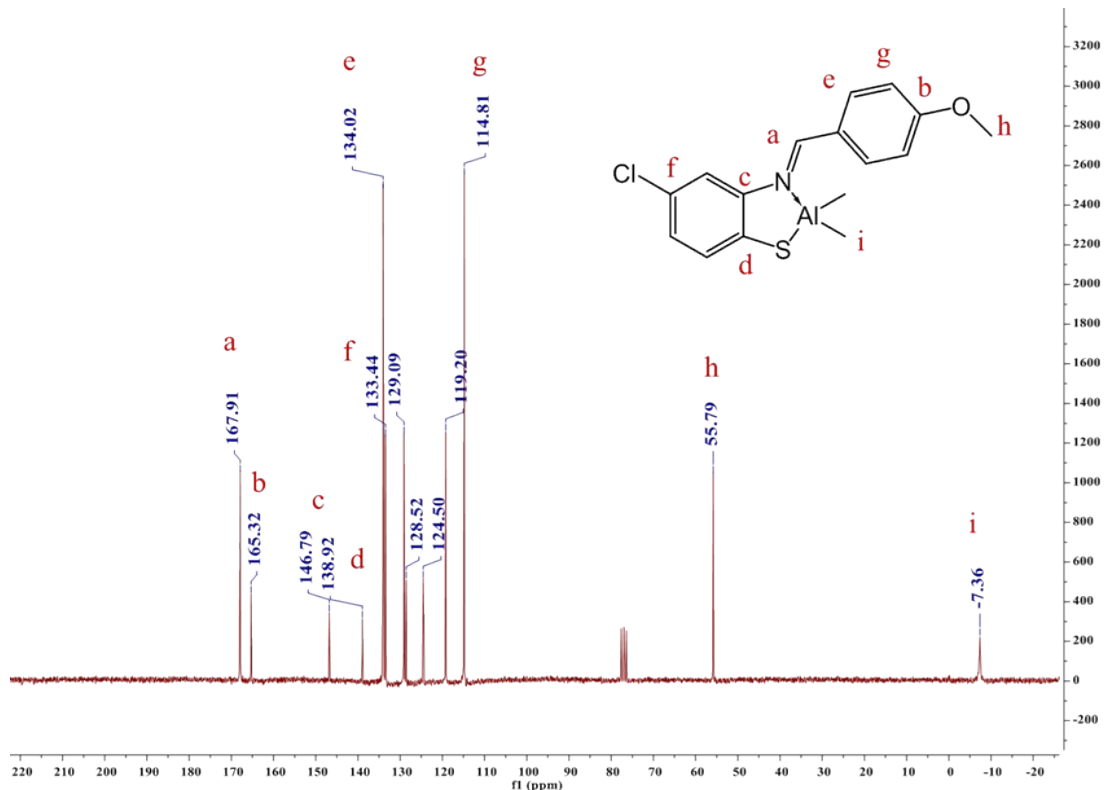


Figure S11. ${}^{13}\text{C}$ NMR spectrum of $\text{L}^{\text{ClO}}\text{AlMe}_2$

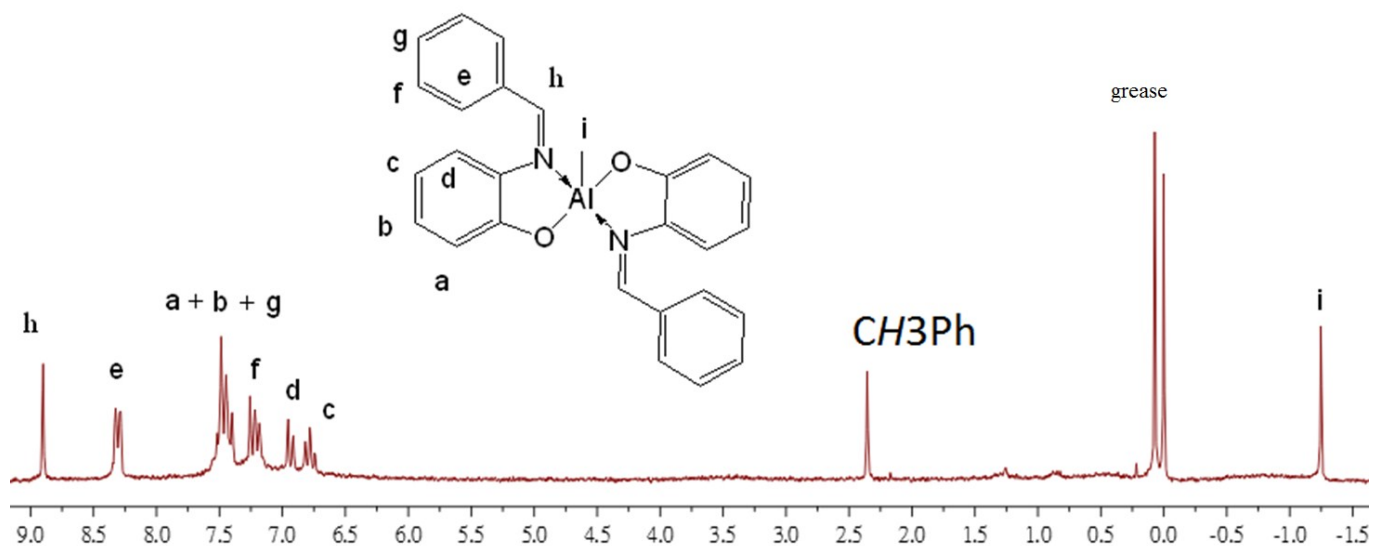


Figure S12. ^1H NMR spectrum of $\text{O}^{\text{H}}_2\text{AlMe}$

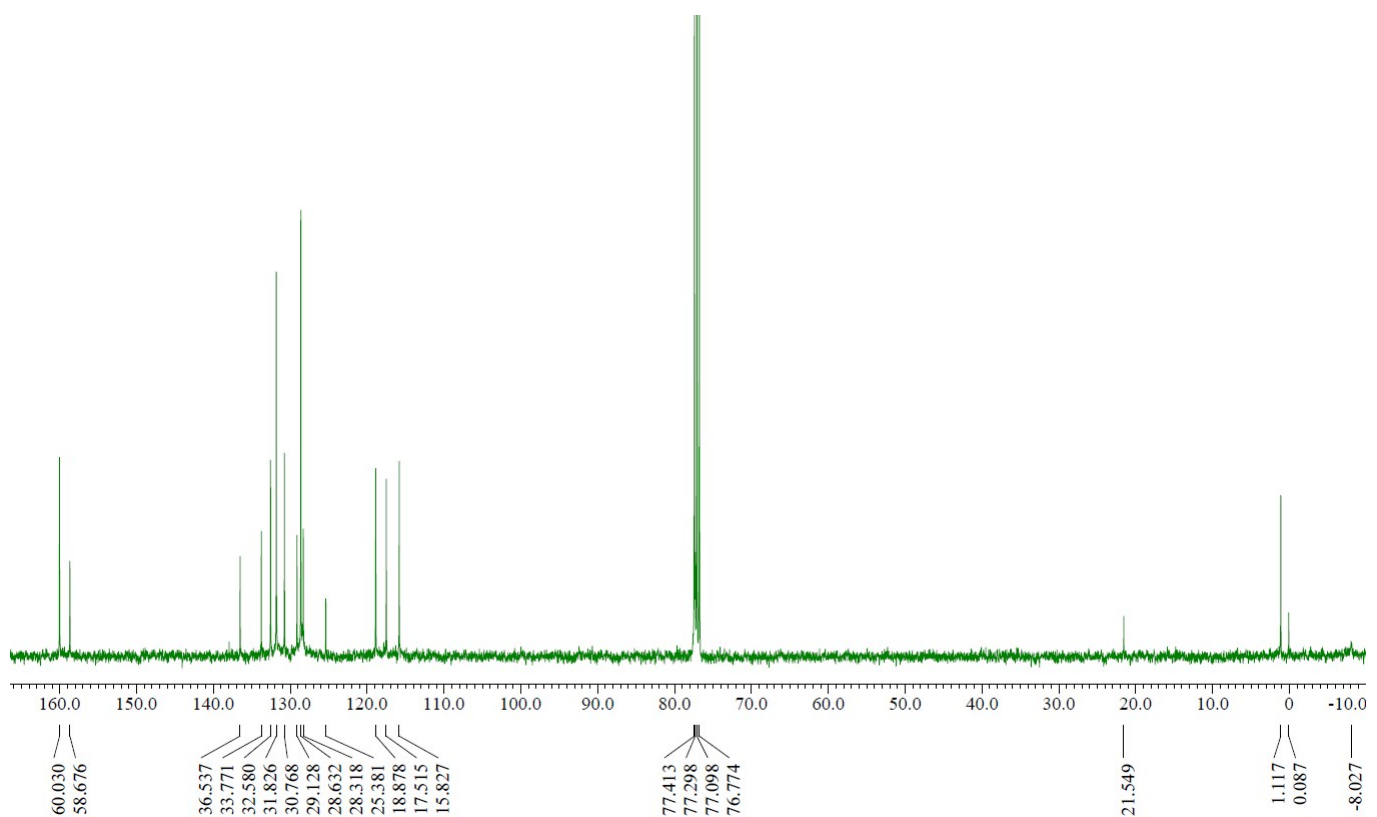


Figure S13. ^{13}C NMR spectrum of $\text{O}^{\text{H}}_2\text{AlMe}$

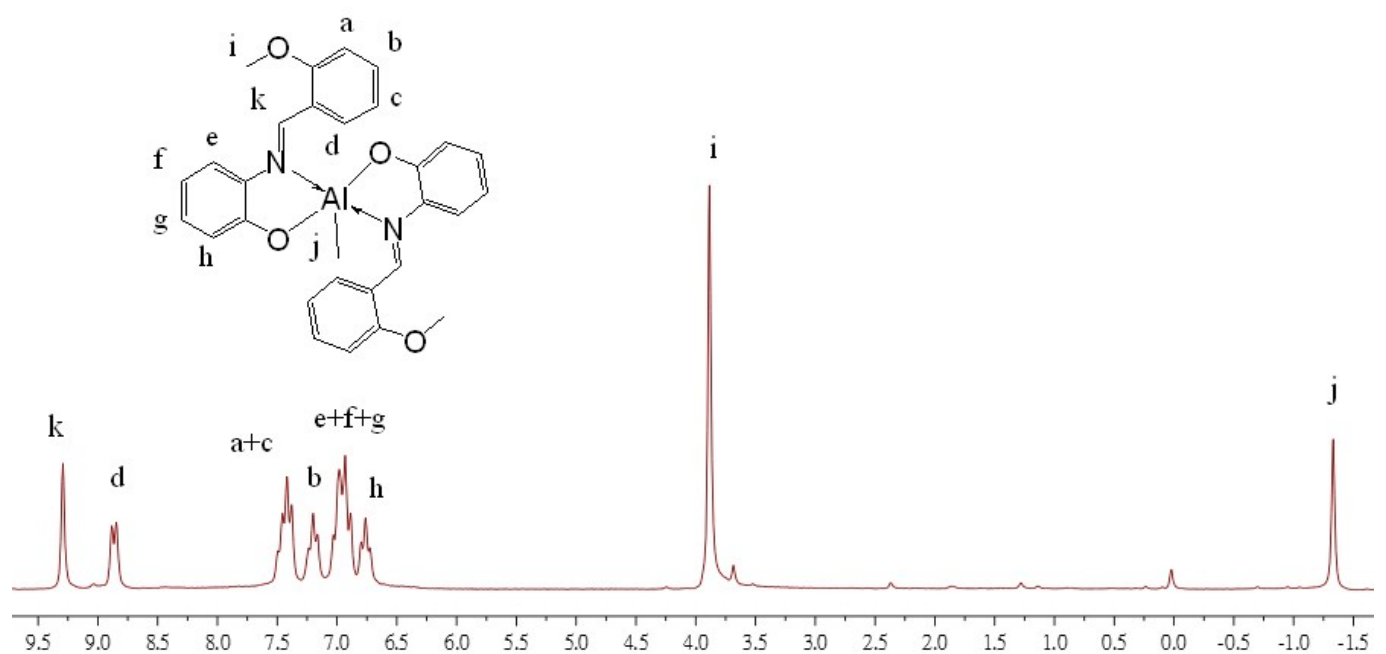


Figure S14. ^1H NMR spectrum of $\text{O}^{\text{OMe}_2}\text{AlMe}$

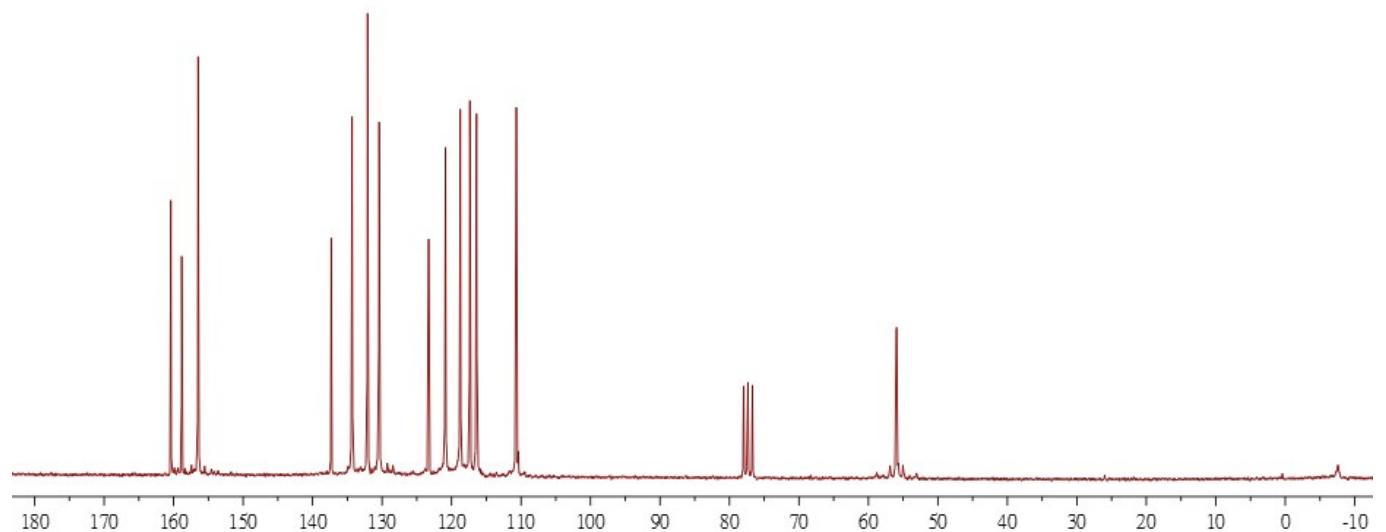


Figure S15. ^{13}C NMR spectrum of $\text{O}^{\text{OMe}_2}\text{AlMe}$

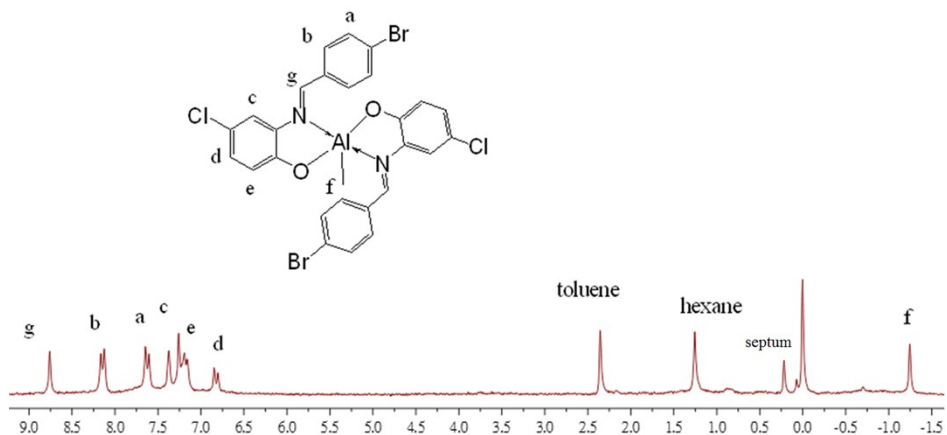


Figure S16. ^1H NMR spectrum of $\text{OClBr}_2\text{AlMe}$

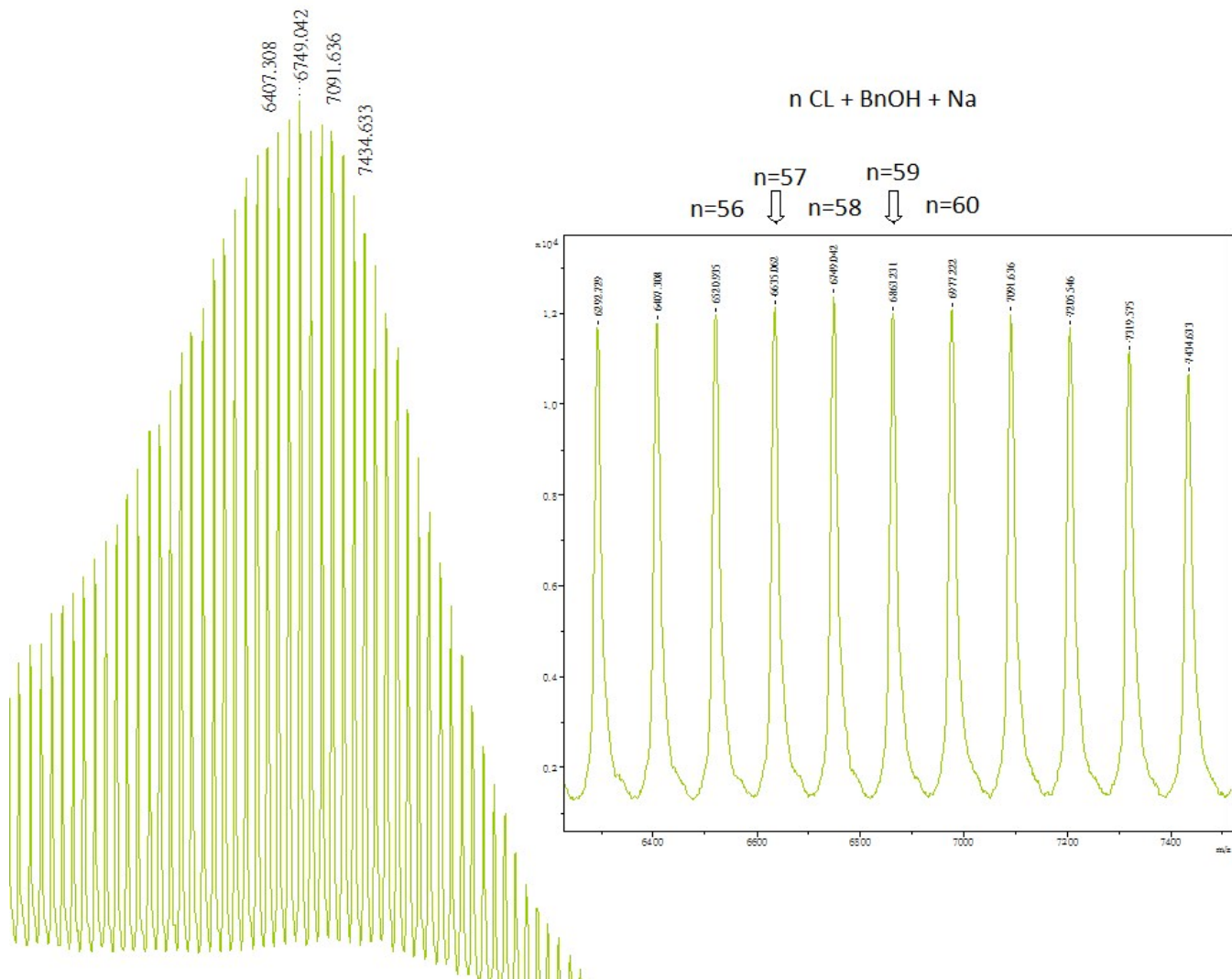


Figure S17. MALDI-TOF spectrum of PCL (matrix: DCTB; ionization salt: NaI; solvent: CH_2Cl_2 , entry 9, Table 3)

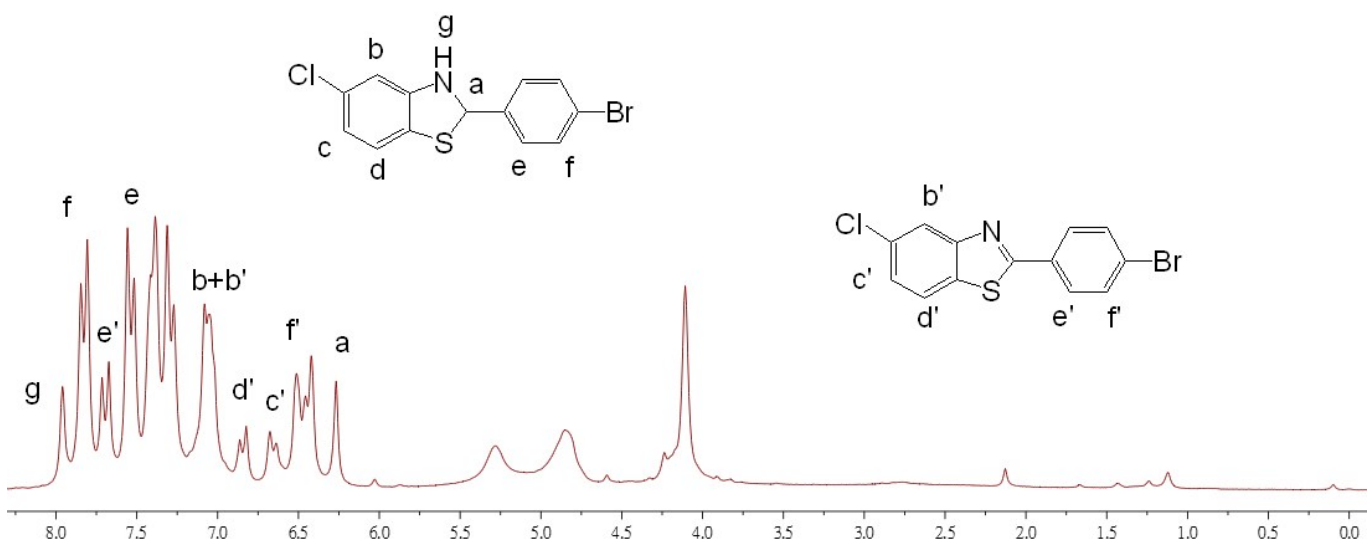


Figure S18. ^1H NMR spectrum of $\text{L}^{\text{ClBr}}\text{-H}$ and 2-(4-bromophenyl)-5-chlorobenzothiazole

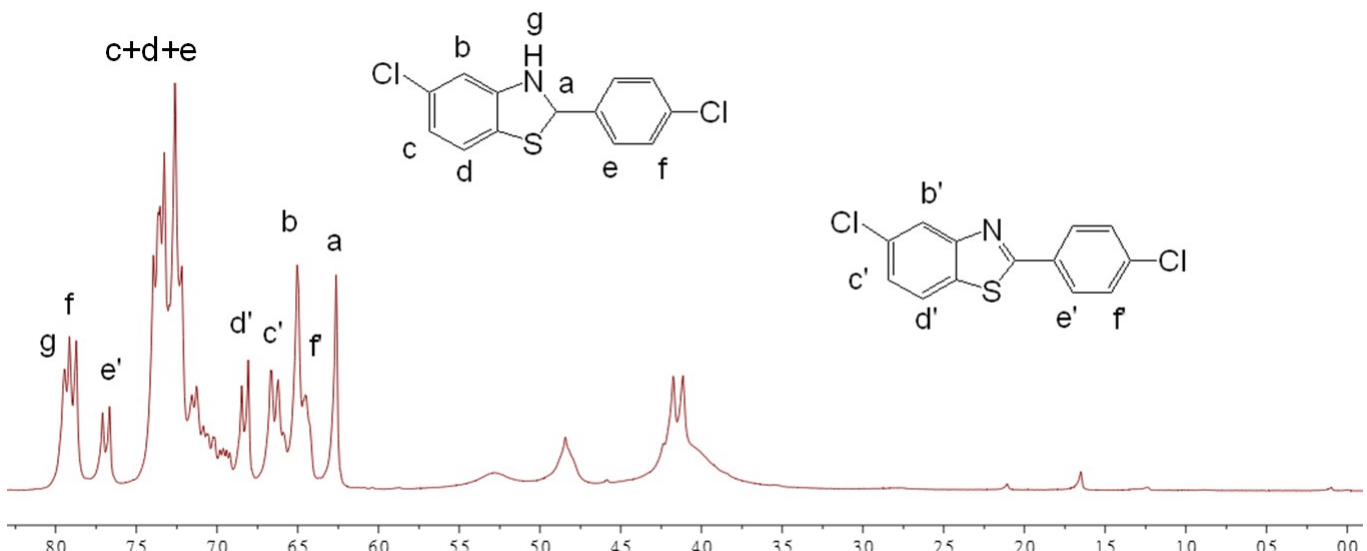


Figure S19. ^1H NMR spectrum of $\text{L}^{\text{ClCl}}\text{-H}$ and 2-(4-chlorophenyl)-5-chlorobenzothiazole

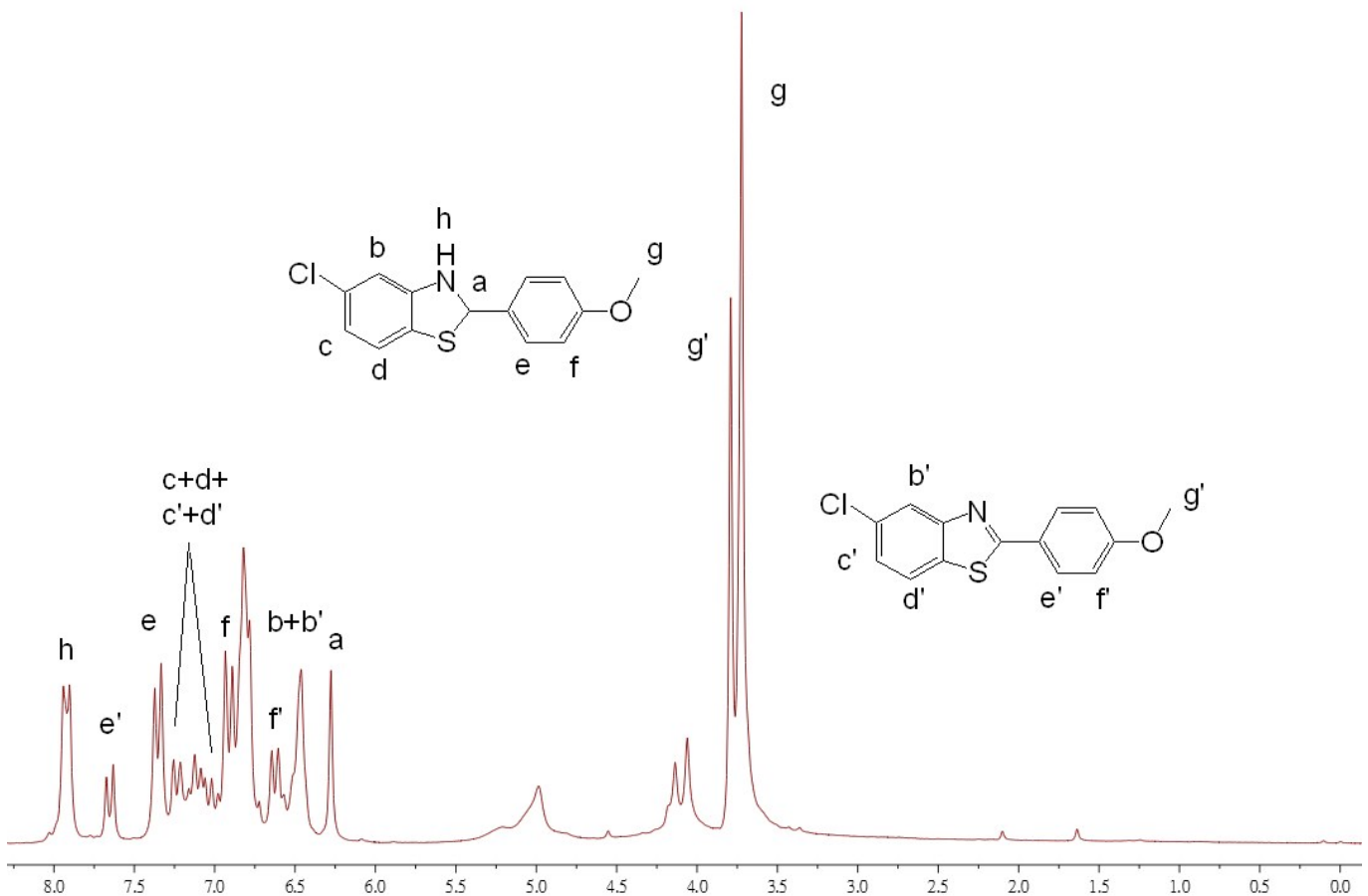


Figure S20. ^1H NMR spectrum of $\text{L}^{\text{ClO}}\text{-H}$ and 5-chloro-2-(4-methoxyphenyl)benzothiazole

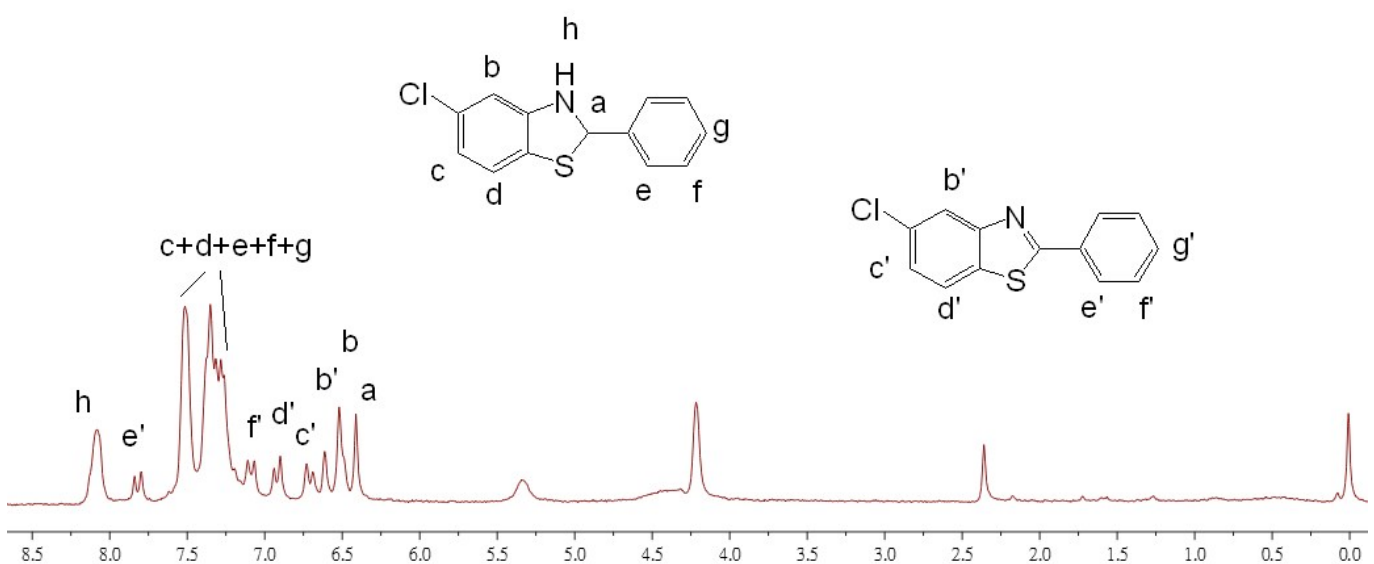


Figure S21. ^1H NMR spectrum of $\text{L}^{\text{ClH}}\text{-H}$ and 5-chloro-2-phenylbenzothiazole

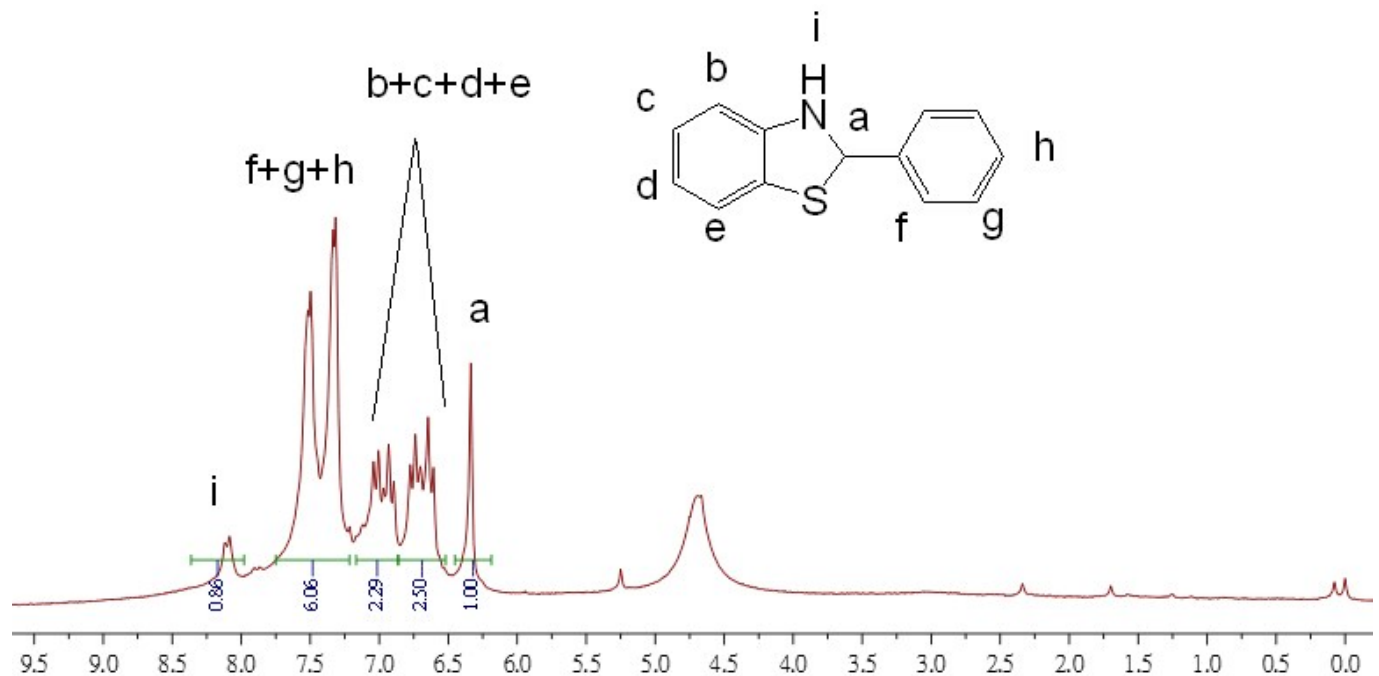


Figure S22. ${}^1\text{H}$ NMR spectrum of $\mathbf{L}^{\text{HH}}\text{-H}$ and 2-phenylbenzothiazole

Table S3. Crystal data and structure refinement for **L^{ClH}AlMe₂ (4)**.

Identification code	d19159	
Empirical formula	C15 H15 Al Cl N S	
Formula weight	303.77	
Temperature	200(2) K	
Wavelength	0.71073 Å	
Crystal system	Monoclinic	
Space group	P 21/c	
Unit cell dimensions	a = 11.8748(9) Å b = 12.7887(10) Å c = 11.2417(7) Å	a= 90°. b= 117.102(2)°. g = 90°.
Volume	1519.74(19) Å ³	
Z	4	
Density (calculated)	1.328 Mg/m ³	
Absorption coefficient	0.432 mm ⁻¹	
F(000)	632	
Crystal size	0.42 x 0.20 x 0.08 mm ³	
Theta range for data collection	2.50 to 25.05°.	
Index ranges	-12<=h<=14, -15<=k<=15, -13<=l<=13	
Reflections collected	28773	
Independent reflections	2685 [R(int) = 0.0570]	
Completeness to theta = 25.05°	99.8 %	
Absorption correction	multi-scan	
Max. and min. transmission	0.9663 and 0.8395	
Refinement method	Full-matrix least-squares on F ²	
Data / restraints / parameters	2685 / 0 / 173	
Goodness-of-fit on F ²	1.038	
Final R indices [I>2sigma(I)]	R1 = 0.0324, wR2 = 0.0753	
R indices (all data)	R1 = 0.0429, wR2 = 0.0816	
Largest diff. peak and hole	0.246 and -0.251 e.Å ⁻³	

Table S4. Atomic coordinates ($\times 10^4$) and equivalent isotropic displacement parameters ($\text{\AA}^2 \times 10^3$) for $\mathbf{L}^{\text{ClH}}\text{AlMe}_2$ (4). U(eq) is defined as one third of the trace of the orthogonalized U_{ij}^{eq} tensor.

	x	y	z	U(eq)
C(1)	7848(2)	3691(2)	6293(2)	35(1)
C(2)	6480(2)	1474(2)	6723(2)	39(1)
C(3)	3604(2)	3318(2)	4416(2)	28(1)
C(4)	2320(2)	3231(2)	3528(2)	34(1)
C(5)	1404(2)	3396(2)	3935(2)	36(1)
C(6)	1761(2)	3647(2)	5253(2)	31(1)
C(7)	3015(2)	3758(1)	6161(2)	27(1)
C(8)	3935(2)	3613(1)	5735(2)	24(1)
C(9)	5585(2)	4386(1)	7592(2)	26(1)
C(10)	6839(2)	4499(1)	8700(2)	25(1)
C(11)	7173(2)	5454(2)	9366(2)	35(1)
C(12)	8344(2)	5587(2)	10443(2)	44(1)
C(13)	9189(2)	4768(2)	10886(2)	42(1)
C(14)	8864(2)	3811(2)	10258(2)	36(1)
C(15)	7696(2)	3672(2)	9171(2)	29(1)
Al(1)	6351(1)	2896(1)	6042(1)	25(1)
Cl(1)	611(1)	3796(1)	5796(1)	46(1)
N(1)	5255(1)	3708(1)	6641(1)	23(1)
S(1)	4776(1)	3081(1)	3900(1)	38(1)

Table S5. Bond lengths [\AA] and angles [$^\circ$] for $\mathbf{L}^{\text{ClH}}\mathbf{AlMe}_2$ (**4**).

C(1)-Al(1)	1.953(2)
C(1)-H(1A)	0.9800
C(1)-H(1B)	0.9800
C(1)-H(1C)	0.9800
C(2)-Al(1)	1.951(2)
C(2)-H(2A)	0.9377
C(2)-H(2B)	0.9150
C(2)-H(2C)	0.8880
C(3)-C(4)	1.395(3)
C(3)-C(8)	1.401(3)
C(3)-S(1)	1.761(2)
C(4)-C(5)	1.375(3)
C(4)-H(4)	0.9500
C(5)-C(6)	1.381(3)
C(5)-H(5)	0.9500
C(6)-C(7)	1.376(3)
C(6)-Cl(1)	1.741(2)
C(7)-C(8)	1.392(3)
C(7)-H(7)	0.9500
C(8)-N(1)	1.433(2)
C(9)-N(1)	1.290(2)
C(9)-C(10)	1.449(3)
C(9)-H(9)	0.9500
C(10)-C(11)	1.393(3)
C(10)-C(15)	1.394(3)
C(11)-C(12)	1.376(3)
C(11)-H(11)	0.9500
C(12)-C(13)	1.377(3)
C(12)-H(12)	0.9500
C(13)-C(14)	1.377(3)
C(13)-H(13)	0.9500
C(14)-C(15)	1.380(3)
C(14)-H(14)	0.9500
C(15)-H(15)	0.9500
Al(1)-N(1)	2.0074(16)
Al(1)-S(1)	2.2904(8)
Al(1)-C(1)-H(1A)	109.5

Al(1)-C(1)-H(1B)	109.5
H(1A)-C(1)-H(1B)	109.5
Al(1)-C(1)-H(1C)	109.5
H(1A)-C(1)-H(1C)	109.5
H(1B)-C(1)-H(1C)	109.5
Al(1)-C(2)-H(2A)	116.9
Al(1)-C(2)-H(2B)	119.1
H(2A)-C(2)-H(2B)	110.8
Al(1)-C(2)-H(2C)	112.3
H(2A)-C(2)-H(2C)	104.7
H(2B)-C(2)-H(2C)	88.4
C(4)-C(3)-C(8)	117.88(19)
C(4)-C(3)-S(1)	121.34(15)
C(8)-C(3)-S(1)	120.78(15)
C(5)-C(4)-C(3)	121.43(19)
C(5)-C(4)-H(4)	119.3
C(3)-C(4)-H(4)	119.3
C(4)-C(5)-C(6)	119.38(19)
C(4)-C(5)-H(5)	120.3
C(6)-C(5)-H(5)	120.3
C(7)-C(6)-C(5)	121.25(19)
C(7)-C(6)-Cl(1)	119.03(16)
C(5)-C(6)-Cl(1)	119.70(16)
C(6)-C(7)-C(8)	119.02(18)
C(6)-C(7)-H(7)	120.5
C(8)-C(7)-H(7)	120.5
C(7)-C(8)-C(3)	120.96(17)
C(7)-C(8)-N(1)	121.29(16)
C(3)-C(8)-N(1)	117.68(17)
N(1)-C(9)-C(10)	125.72(17)
N(1)-C(9)-H(9)	117.1
C(10)-C(9)-H(9)	117.1
C(11)-C(10)-C(15)	118.77(18)
C(11)-C(10)-C(9)	118.60(17)
C(15)-C(10)-C(9)	122.52(17)
C(12)-C(11)-C(10)	120.5(2)
C(12)-C(11)-H(11)	119.8
C(10)-C(11)-H(11)	119.8
C(11)-C(12)-C(13)	120.2(2)
C(11)-C(12)-H(12)	119.9

C(13)-C(12)-H(12)	119.9
C(12)-C(13)-C(14)	120.14(19)
C(12)-C(13)-H(13)	119.9
C(14)-C(13)-H(13)	119.9
C(13)-C(14)-C(15)	120.17(19)
C(13)-C(14)-H(14)	119.9
C(15)-C(14)-H(14)	119.9
C(14)-C(15)-C(10)	120.25(18)
C(14)-C(15)-H(15)	119.9
C(10)-C(15)-H(15)	119.9
C(2)-Al(1)-C(1)	121.65(10)
C(2)-Al(1)-N(1)	107.32(8)
C(1)-Al(1)-N(1)	111.62(8)
C(2)-Al(1)-S(1)	112.90(8)
C(1)-Al(1)-S(1)	110.58(7)
N(1)-Al(1)-S(1)	87.46(5)
C(9)-N(1)-C(8)	117.85(16)
C(9)-N(1)-Al(1)	128.84(13)
C(8)-N(1)-Al(1)	112.54(11)
C(3)-S(1)-Al(1)	93.50(7)

Symmetry transformations used to generate equivalent atoms:

Table S6. Anisotropic displacement parameters ($\text{\AA}^2 \times 10^3$) for d19159. The anisotropic displacement factor exponent takes the form: $-2p^2 [h^2 a^*^2 U^{11} + \dots + 2 h k a^* b^* U^{12}]$

	U11	U22	U33	U23	U13	U12
C(1)	36(1)	35(1)	42(1)	-4(1)	24(1)	-6(1)
C(2)	54(2)	26(1)	51(1)	0(1)	36(1)	1(1)
C(3)	32(1)	24(1)	26(1)	-1(1)	13(1)	-3(1)
C(4)	36(1)	32(1)	26(1)	1(1)	6(1)	-5(1)
C(5)	26(1)	31(1)	38(1)	8(1)	4(1)	-4(1)
C(6)	25(1)	25(1)	44(1)	11(1)	16(1)	2(1)
C(7)	28(1)	25(1)	29(1)	3(1)	13(1)	2(1)
C(8)	24(1)	20(1)	25(1)	2(1)	9(1)	-1(1)
C(9)	27(1)	25(1)	26(1)	0(1)	13(1)	2(1)
C(10)	28(1)	26(1)	23(1)	-1(1)	13(1)	-1(1)
C(11)	40(1)	26(1)	30(1)	-3(1)	10(1)	3(1)
C(12)	51(2)	28(1)	36(1)	-7(1)	5(1)	-9(1)
C(13)	36(1)	40(1)	32(1)	3(1)	1(1)	-9(1)
C(14)	31(1)	36(1)	33(1)	7(1)	8(1)	5(1)
C(15)	33(1)	26(1)	28(1)	-2(1)	13(1)	-2(1)
Al(1)	27(1)	24(1)	28(1)	-2(1)	17(1)	-2(1)
Cl(1)	29(1)	49(1)	64(1)	17(1)	26(1)	8(1)
N(1)	23(1)	23(1)	22(1)	1(1)	10(1)	0(1)
S(1)	39(1)	52(1)	25(1)	-7(1)	16(1)	-1(1)

Table S7. Hydrogen coordinates ($\times 10^4$) and isotropic displacement parameters ($\text{\AA}^2 \times 10^3$) for $\mathbf{L}^{\text{ClH}}\text{AlMe}_2$ (4).

	x	y	z	U(eq)
H(1A)	8595	3402	7049	53
H(1B)	7741	4425	6473	53
H(1C)	7958	3646	5481	53
H(2A)	6338	1384	7471	47
H(2B)	6134	936	6130	47
H(2C)	7237	1196	6958	47
H(4)	2074	3055	2622	41
H(5)	534	3338	3315	43
H(7)	3249	3930	7066	33
H(9)	4950	4852	7562	31
H(11)	6588	6018	9076	42
H(12)	8570	6244	10882	53
H(13)	9999	4864	11626	50
H(14)	9445	3245	10574	43
H(15)	7476	3010	8741	35